

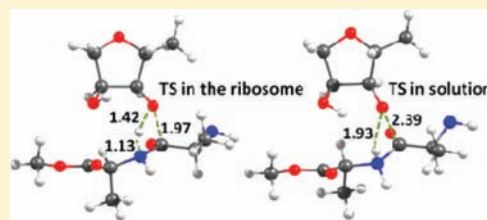
Quantum-Mechanical Study on the Mechanism of Peptide Bond Formation in the Ribosome

Carles Acosta-Silva, Joan Bertran,* Vicenç Branchadell, and Antoni Oliva

Departament de Química, Universitat Autònoma de Barcelona, 08193 Bellaterra, Spain

S Supporting Information

ABSTRACT: Ribosomes transform the genetic information encoded within genes into proteins. In recent years, there has been much progress in the study of this complex molecular machine, but the mechanism of peptide bond formation and the origin of the catalytic power of this ancient enzymatic system are still an unsolved puzzle. A quantum-mechanical study of different possible mechanisms of peptide synthesis in the ribosome has been carried out using the M06-2X density functional. The uncatalyzed processes in solution have been treated with the SMD solvation model. Concerted and two-step mechanisms have been explored. Three main points suggested in this work deserve to be deeply analyzed. First, no zwitterionic intermediates are found when the process takes place in the ribosome. Second, the proton shuttle mechanism is suggested to be efficient only through the participation of the A2451 2'-OH and two crystallographic water molecules. Finally, the mechanisms in solution and in the ribosome are very different, and this difference may help us to understand the origin of the efficient catalytic role played by the ribosome.



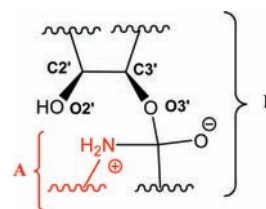
INTRODUCTION

Ribosomes transform the genetic information encoded within genes into proteins.^{1–3} An important advance in the study of this complex molecular machine was reached when crystal structures of the two ribosomal subunits at high resolution (2.4–3.0 Å)^{4–6} and the complete ribosome at 5.5 Å⁷ were obtained. The largest subunit contains the peptidyl transferase center (PTC), which catalyzes the formation of peptide bonds in the growing polypeptide. Since there are no protein side-chain atoms closer than 18 Å to the peptide bond, this implies that the peptidyl transferase (PT) reaction is catalyzed by RNA and, thus, that the ribosome itself acts as a ribozyme.^{8,9} Despite the great progress in the study of the ribosome function in the synthesis of proteins, the mechanism of the process and the origin of the catalytic power of this ancient enzyme are still an unsolved puzzle.

When peptidyl transfer is studied using native substrates, the rate of peptide bond formation is determined by the preceding rate-limiting step of aa-tRNA binding to the A site (accommodation), which is relatively slow. Given that the intrinsic rate of peptide bond formation is much faster than that, moderate changes in the rate of the chemical step are likely to be obscured by the slow binding step. For this reason, substrate analogues, such as puromycin, which do not need to accommodate, are used.^{10,11} Resolution of the structures of A and P site substrate and product analogues as well as an intermediate analogue has been refined.^{12,13} Stabilization of the transition state (TS) of the PT reaction by the ribosome might contribute to catalysis. This possibility has been examined using analogues in which a phosphate diester mimics the tetrahedral TS that occurs during the peptide bond formation.^{14,15}

One suggested mechanism is that the nucleophilic α -amino group of an aminoacyl-tRNA bound to the A site of the PTC attacks the electrophilic carbonyl carbon of the ester bond linking the peptide moiety to the P-site of tRNA. The resulting charged tetrahedral carbon intermediate (Scheme 1) would be

Scheme 1. Zwitterionic Intermediate



stabilized by the interaction with a water molecule which is positioned by two nucleotides.¹⁵ Then, the intermediate rearranges and decomposes to yield deacylated tRNA in the P site and peptidyl-tRNA that is longer by one amino acid in the A site. However, a recent paper¹⁶ argues on the basis of experimental data that the stabilization of the transition structure by the water molecule is quite small.

An alternative mechanism states that the peptide synthesis takes place through general acid–base catalysis, the N3 of A2451 acting as a general base.^{17–20} However, more recent studies show that this mechanism can be disregarded.^{21–23}

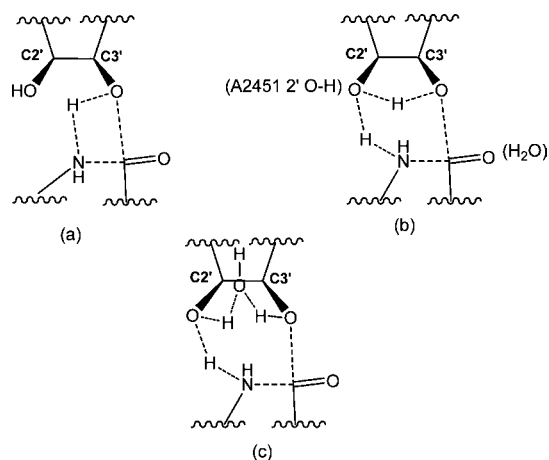
It has been proposed that proton shuttling through one group of the ribosome could also take place through a group of the substrate itself. In particular, the A76 2'-OH of the peptidyl-tRNA

Received: October 11, 2011

Published: March 1, 2012

is hydrogen-bonded to the α -amino group and could facilitate peptide bond formation by acting as a proton shuttle between the α -amino group and the A76 3'-hydroxyl of the peptidyl-tRNA^{15,24–29} (Scheme 2b). Green and Strobel³⁰ reported

Scheme 2. Transition States of the Proposed Concerted Mechanisms: (a) Four-Membered Ring Cycle, (b) Six-Membered Ring Cycle, and (c) Eight-Membered Ring Cycle



experimental evidence of the participation of the substrate itself in the catalytic process. They showed that substitution of the P-site tRNA A76 2'-OH with 2'-H or 2'-F results in at least a 10^6 -fold reduction in the rate of peptide bond formation, but does not affect binding of the modified substrates. So, they conclude that substrate-assisted catalysis, although quite uncommon among modern protein enzymes, is essential for the evolution of enzymatic function, and they suggest that substrate assistance is retained as a catalytic strategy during the evolution of the prebiotic PTC into the modern ribosome. This proton shuttle mechanism was questioned by Sprinzl's group.^{31,32} In a more recent paper, Green and Strobel's group³³ reinvestigated the kinetic contribution of the 2'-OH group to the catalysis and found that it is significantly smaller (~ 100 -fold). These new findings reconcile the conflict in the literature and support a model where interactions between active site residues and the 2'-OH are pivotal in orienting substrates in the active site for optimal catalysis.

According to Schmeing et al.,¹⁵ several catalytic pathways can be envisaged. The α -amino group could nucleophilically attack the ester carbon, forming a zwitterion intermediate, which could break down by the transfer of a H atom from the amino group to the 2'-hydroxyl in concert with its hydrogen being passed to the 3'-hydroxyl leaving group. Alternatively, a concerted mechanism is possible. Finally, the proton shuttle from the attacking α -amino group via the 2'-hydroxyl to the 3'-hydroxyl could include the water molecule that is simultaneously hydrogen-bonded to the 2'-hydroxyl as an acceptor and the 3'-hydroxyl oxygen as a donor (Scheme 2c).

A second 2'-OH group was identified to be crucial for peptide bond formation, namely that of A2451. Interestingly, removal of the entire nucleobase of A2451 nucleotide, leaving the sugar-phosphate backbone intact, does not significantly impair the rate of peptide bond formation. In contrast, the 2'-OH of A2451 was shown to be of potential functional importance.^{34–38} The question of cooperation between the two essential 2'-OH groups during peptide bond formation remained to be clarified. Lang et al.³⁹ showed that the ribose

of the A76 residue of the P-tRNA is kept, due to the interaction with the 2'-OH of A2451, in its RNA-unfavorable C2'-endo configuration, which is important for the proton shuttle (Scheme 2b).

Brønsted linear free energy relationships with slopes close to zero for the PT reaction between the α -amino nucleophile with a series of puromycin derivatives indicate^{40,41} that, in the ribosome-catalyzed reaction, the nucleophile is neutral at the TS, in contrast to the substantial positive charge reported for typical uncatalyzed aminolysis reactions. This suggests that the ribosomal TS involves deprotonation to a degree commensurate with nitrogen-carbon bond formation. The observation of a normal effect for ¹⁵N substitution of the incoming nucleophile and the fact that it does not change as a function of pH suggest that the nitrogen is being deprotonated simultaneously with the formation of the C-N bond, confirming that the ribosome promotes peptide bond formation by a mechanism that differs in its details from an uncatalyzed aminolysis reaction in solution.^{42,44} The same conclusion is reached when kinetic isotope effects of several atoms are measured for the uncatalyzed⁴³ and the ribosome-catalyzed⁴⁴ reaction. Finally, solvent isotope effects and proton inventories indicate that the rate-limiting step is the formation of three hydrogen bonds with about equal contributions, this fact being consistent with a concerted eight-membered proton shuttle in the TS.⁴⁵

To determine the effectiveness of the ribosome as a catalyst, several kinetic studies were carried out.^{46–51} They showed that, in contrast with most protein enzymes, the enthalpy of activation is slightly less favorable on the ribosome than in solution. The 2×10^7 -fold rate enhancement produced by the ribosome is achieved entirely by lowering the entropy of activation. This suggests that the ribosome promotes the reaction of the amino acid condensation by properly orienting the reaction substrates.^{52,53} So, the ribosome acts as an entropic trap⁵⁴ that draws its catalytic power from the ability to orient and position substrates.

To explore the different possible mechanistic alternatives for the ribosomal peptidyl transfer reaction, several authors^{55–58} carried out extensive molecular dynamics (MD) free energy calculations by using the Warshel's empirical valence bond (EVB) method.⁵⁹ They found that a significant part of the observed activation entropy of the reference solution reaction is due to solvation entropy, and that the proximity effect is smaller than previously thought. Trobro and Aqvist^{56,58} stated that catalysis is mainly achieved through a stable network of hydrogen bonds to the reactants that reduces the reorganization energy and the activation entropy of the reaction. This predicted hydrogen-bonding network, including positions of key solvent molecules and the stereochemical route of the peptidyl transfer reaction, was verified in crystal structures with TS analogues.¹⁵

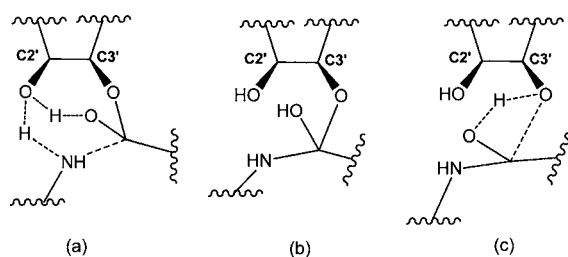
The mechanism of protein synthesis in the ribosome has also been the subject of several quantum-mechanical (QM) studies.^{60–67} These studies obviously imply the use of a reduced model for the system. The pioneering work was that of Das et al.⁶⁰ in which semiempirical methods were used to study the energetics for the formation of a cyclic intermediate; the authors concluded that the peptide bond formation through the tetrahedral intermediate in *S* configuration may not need assistance from any outside agent, like an enzyme. In a second work, Suárez et al.,⁶¹ using DFT at the B3LYP level, gave support to the idea that the activated nucleotide A2451 in the ribosome acts as a base catalyst and that its role is similar to

that of the His residue in the catalytic triad of serine proteases. In more recent papers, Yonath's group studied^{62,63} the attack of the α -NH₂ group to the ester carbon, which is accompanied by the transfer of a proton from NH₂ to the O3' oxygen (Scheme 2a) for a reduced model with 50 atoms at the B3LYP level. They showed that the four-ring cyclic TS is formed with a simultaneous rotation which enables the translocation of the A-site tRNA 3' end into the P site. The calculated activation energy is 35.5 kcal/mol, and the increase in hydrogen bonding between the rotating A-site tRNA and ribosome nucleotides stabilizes the TS by a value of \sim 18 kcal/mol. In this mechanism, the 2'-OH is not involved in proton transfer, its role being to act as an anchor to hold the reactant. Thirumoorthy et al.⁶⁴ found that the energy barrier for this anchoring mechanism is \sim 2 kcal/mol lower than the one corresponding to the shuttle mechanism at the HF/3-21G level of theory.

Recently, Wallin et al.⁶⁵ studied the shuttle mechanism with the formation of six- and eight-membered rings at the B3LYP level. They started from representative snapshots of their previous MD simulations to localize the corresponding TSs. The calculated activation enthalpies, as well as the structures, are in good agreement with experimental data and point to the feasibility of an eight-membered "double proton shuttle" mechanism (Scheme 2c), in which an auxiliary water molecule actively participates. A second conserved water molecule is found to be of key importance for stabilizing the developing negative charge on the substrate oxyanion. Transition states calculated for both six- and eight-membered rings are invariably late and do not involve substantial charge development in the attacking amino group. One can conclude that the rRNA is folded in a rather inert structure that does not directly participate in the chemistry, but it provides key interactions to those groups that are directly involved in the reaction. It might seem surprising that the only active groups are the A2451 2'-OH and two "trapped" water molecules.

Wang et al.,⁶⁶ following an idea of Rangelov et al.,⁶⁷ carried out a B3LYP study of a two-step mechanism (Scheme 3) in

Scheme 3. Two-Step Mechanism: (a) First Transition State, (b) Intermediate, and (c) Second Transition State



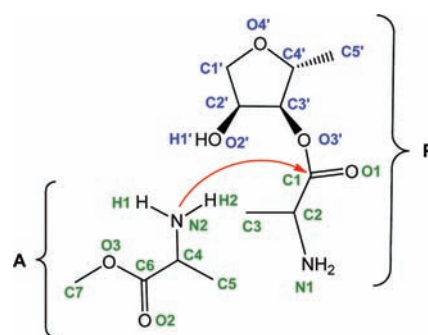
which the A76 2'-OH group transfers one proton to the carbonyl O atom while, simultaneously, it receives one proton from the α -NH₂ group (Scheme 3a). Protonation of the carbonyl oxygen neutralizes the negative charge of the oxyanion, leading to a neutral intermediate (Scheme 3b). In a second step, the proton is transferred to the O3' leaving group (Scheme 3c). The energy barrier of the first step amounts to 24.0 kcal/mol. The TS is a six-membered ring, as in one of the shuttle mechanisms, but involving a different O atom. In the second step, the intermediate decomposes to products through an energy barrier of 13.1 kcal/mol via a four-membered ring TS.

The above-mentioned QM studies have been done with different methods and different basis sets. The purpose of this paper is to carry out a more complete study of the proposed mechanisms of peptide synthesis in the ribosome using a more recent DFT functional and a larger basis set, overcoming some of the limitations of previous works. The use of a common method in all mechanisms will allow us to make a more reliable comparative study of them.

COMPUTATIONAL METHODS

As mentioned above, the QM study of a complex system implies the use of a reduced model. Scheme 4 shows the model which is adopted

Scheme 4. Schematic Drawing Showing the Reactants in the Nucleophilic Attack of the Amino Group of Aminoacyl tRNA at the A-Site on the Carbonyl Group of the Ester Formed between the Peptide Chain and tRNA at the P-Site^a

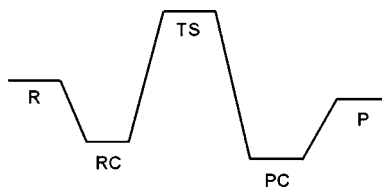


^aThis numbering of the atoms will be used throughout the paper.

in this work. Our model includes all the atoms that intervene in the different proposed mechanisms. The main simplifications we did can be summarized as follows. The atom C5', which in the real system is bonded to the O atom of a phosphate in the RNA main chain, is represented by a methyl group. The base bonded to the C1' is modeled by a H atom. The methyl groups C3 and C5 act as a model of the lateral chain of an amino acid. In the amino group N1, one of the H atoms takes the place of a polypeptide chain. Finally, the C7 methyl group models the ribose of tRNA at the A-site. Only the three H atoms which intervene in the process are explicitly shown and numerated. When necessary, the 2-OH of A2451 and the two trapped water molecules mentioned in the Introduction will be explicitly considered in the philosophy of the theozymes (theoretical enzymes) proposed by Tantillo et al.⁶⁸

The strategy we adopted to study the process is the following. We started from reasonable structures of the four-, six-, and eight-membered rings of the proposed TSs, and we optimized the rest of the geometry parameters. From these structures, we located the TSs. For each TS the intrinsic reaction coordinate⁶⁹ (IRC) was calculated. The final points of each reaction path are used to fully characterize the reactant and product complexes associated with each TS. Finally, the isolated reactants and products are optimized.

In past years, the B3LYP functional⁷⁰ has been usually employed, although it is not suitable for large systems, in which dispersion energy plays an important role. To solve this inconsistency, we decided to use the M06-2X functional proposed by Truhlar's group,^{71,72} a highly parametrized metahybrid method which has shown to be very adequate for the study of non-covalent interactions, especially hydrogen bonds. Several authors emphasized the good performance of this functional in the study of different thermochemistry and kinetics problems and non-covalent interactions when comparing their results to those in benchmark databases.^{73–81} Single-point MP2 calculations were also carried out for all the stationary points. All the calculations were done using the triple- ζ 6-311+G(d,p) basis set. Truhlar^{82–84} showed that this basis set is very adequate when using the

Table 1. Summary of Energies (kcal/mol) at the M06-2X/6-311+G(d,p) Level of Calculation for the One-Step Mechanisms^a

mechanism	energy	R	RC	TS	PC	P
I-4	ΔE	0.0	-6.65 (-7.39)	30.11 (25.83)	-15.43 (-16.06)	-2.93 (-2.46)
	ΔH	0.0	-4.86	28.51	-13.93	-2.52
	ΔG	0.0	7.15	42.82	-1.25	-1.61
I-6	ΔE	0.0	-8.95 (-9.13)	33.30 (26.76)	-16.28 (-16.81)	-5.26 (-4.99)
	ΔH	0.0	-7.18	30.36	-14.69	-5.29
	ΔG	0.0	5.03	46.50	-2.36	-6.05
I-8	ΔE	0.0	-10.42 (-10.61)	24.57 (21.06)	-16.83 (-17.80)	-5.01 (-3.96)
	ΔH	0.0	-8.31	22.68	-14.93	-4.56
	ΔG	0.0	5.14	38.41	-1.76	-4.26
I-6wm	ΔE	0.0	-16.25 (-16.29)	28.09 (21.85)	-25.22 (-25.87)	-2.10 (-1.81)
	ΔH	0.0	-14.64	25.71	-23.27	-2.13
	ΔG	0.0	-1.52	43.70	-8.21	-3.25
I-wwm	ΔE	0.0	-9.94 (-9.69)	21.93 (17.91)	-9.64 (-11.32)	6.69 (6.50)
	ΔH	0.0	-8.22	19.91	-8.28	6.21
	ΔG	0.0	5.09	36.53	3.94	2.13

^aValues in parentheses correspond to the MP2/6-311+G(d,p)//M06-2X/6-311+G(d,p) level of calculation.

M06-2X functional and that the inclusion of additional diffuse functions is not necessary.

Introduction of the solvent effect was carried out using the SMD method of Marenich et al.⁸⁵ SMD is a universal solvation model, where “universal” denotes its applicability to any charged or uncharged solute in any solvent or liquid medium for which a few key descriptors are known. In SMD, “D” stands for “density” to denote that the full solute electron density is used without defining partial atomic charges, as was the case in the previous SM8 method.⁸⁶ The SMD model separates the observable solvation free energy into two components: (i) the long-range bulk electrostatic contribution arising from a self-consistent reaction field treatment that involves solution of the nonhomogeneous Poisson equation for electrostatics in terms of the integral equation-formalism polarizable continuum model, and (ii) the cavity dispersion-solvent structure term, which arises from short-range interactions between the solute and solvent molecules in the first solvation shell.

Thermochemical corrections to the energy values were computed using the standard rigid rotor/harmonic oscillator formulas.⁸⁷ Relative Gibbs energies in solution were computed using as the reference state 1 mol L⁻¹ at a temperature of 298.15 K.

All QM calculations were performed through the Gaussian 09 package,⁸⁸ and the stationary points were fully characterized. Full Natural Bond Orbital analysis was carried out with NBO version 3.⁸⁹ Finally, the conformational analysis of the sugar ring in nucleosides was described using the concept of pseudorotation.⁹⁰

RESULTS

As stated in the Introduction, two different kinds of mechanisms are proposed in QM calculations: one-step mechanisms (denoted as I) and two-step mechanisms through an intermediate (denoted

as II). We first present the results corresponding to the one-step mechanisms. In each case, the energy values, the geometry parameters of the stationary points, and the analysis of the charge distribution are successively discussed.

One-Step Mechanisms. *In the Ribosome.* Table 1 shows the variation, with respect to the isolated reactants (R), of the potential energy, the enthalpy, and the Gibbs free energy corresponding to the RC (RC), the transition state (TS), the product complex (PC), and the isolated products (P) for each of the five studied mechanisms. The optimizations were done using the M06-2X functional. For each stationary point, MP2//M06-2X calculations were also done. The first three mechanisms are depicted in Scheme 2: they proceed via a four-membered ring cycle (Scheme 2a), a six-membered ring cycle (Scheme 2b), and an eight-membered ring cycle (Scheme 2c). These mechanisms will be hereafter named I-4, I-6, and I-8, respectively. In the case of the six-membered ring cycle, the inclusion of a methanol molecule and a water molecule, which form hydrogen bonds with the O2' and the O1 oxygen atoms, respectively (see Schemes 2 and 4), was also considered (mechanism I-6wm). The inclusion of a second water molecule in the last mechanism was also studied (mechanism I-wwm). It is worth mentioning that, in the case of the four-membered ring cycle (mechanism I-4), anchoring of the reactant through the formation of a hydrogen bond between the O2'-H1' hydroxyl of the sugar and the carbonylic O2 atom of the nucleophile^{62,63}

was not imposed since this constraint increases the energy barrier by ~ 3 kcal/mol.

Regarding the energy barriers of the bimolecular processes, one can observe that the one of mechanism I-6 (33.3 kcal/mol) is ~ 3 kcal/mol higher than that of mechanism I-4 (30.1 kcal/mol), implying that the substrate-assisted catalysis is not working. In contrast, the inclusion of one water molecule to permit the formation of an eight-membered ring cycle (mechanism I-8) is really efficient, the energy barrier (24.6 kcal/mol) decreasing by ~ 5.5 kcal/mol with respect to that for the four-membered cycle (and ~ 8.7 kcal/mol with respect to the six-membered one). When a methanol molecule and a water molecule are added to the six-membered ring mechanism I-6 (mechanism I-6wm), the energy barrier (28.1 kcal/mol) decreases by ~ 5 kcal/mol and becomes lower than the barrier for the mechanism I-4. However, this lowering of the energy barrier is accompanied by a large stabilization of the RC due to the formation of a hydrogen bond between the C2' hydroxyl group of the sugar and the nucleophilic N atom. This artificial stabilization of the RC is avoided by the addition of a second water molecule (mechanism I-wwm), which leads to an additional decrease of the energy barrier (21.9 kcal/mol) by ~ 6.2 kcal/mol. The activation enthalpy corresponding to the latter mechanism (19.9 kcal/mol) agrees quite well with the experimental value (17 kcal/mol) reported by Johansson et al.⁵¹ This good agreement is still better if one considers the MP2 barriers which are lower than the M06-2X ones, but keeping the ordering unchanged. The Gibbs free energy barriers are 14–18 kcal/mol higher than the enthalpy barrier, in good agreement with the expected negative value of the entropy terms. However, it has to be emphasized that most of this increase (between 11.5 and 13.5 kcal/mol) comes from the formation of the RC, which implies the conversion of six translational and rotational degrees of freedom into vibrations and pseudorotations. The high value of the entropy term suggests that the free energy of the RC is higher than that of the R, in such a way that this complex would not be formed. This can be surprising since the RC is expected to play the role of the Michaelis complex, which, as is well known, is thermodynamically stable. As we have used a simplified model, our results support the idea that the real ribosome acts as an entropic trap that draws its catalytic power from the ability to orient and position substrates.^{52–54}

Figure 1 presents the geometries of the TSs corresponding to the five mechanisms considered in Table 1. There are four bond lengths which play an important role in all the studied mechanisms: the breaking of the N2–H1 and C1–O3' bonds and the formation of the N2–C1 and O3'–H bonds (see Scheme 4 for the numbering of atoms). In the TSs of the mechanisms in the ribosome, the N2–H1 bond length increases from 1.02 Å in R to values between 1.07 and 1.17 Å, the ordering of this bond length being exactly the same as that of the energy barriers. The breaking of the N2–H1 bond is accompanied by the simultaneous bonding of N2 to the C1 atom, the bond lengths ranging 1.51–1.58 Å (the N2–C1 bond length being 1.35–1.38 Å in P). At the same time, the C1–O3' bond is breaking (its bond length having increased from 1.33–1.35 Å in R to 1.84–2.18 Å in TS) and the O3' atom bonds to a H atom (its bond length lying in the range 1.12–1.42 Å), while the values in P are 0.96–0.97 Å. Special attention should be given to mechanism I-wwm, which differs from mechanism I-6wm in a water molecule that makes the formation of an eight-membered ring possible. Figure 1 shows that the located

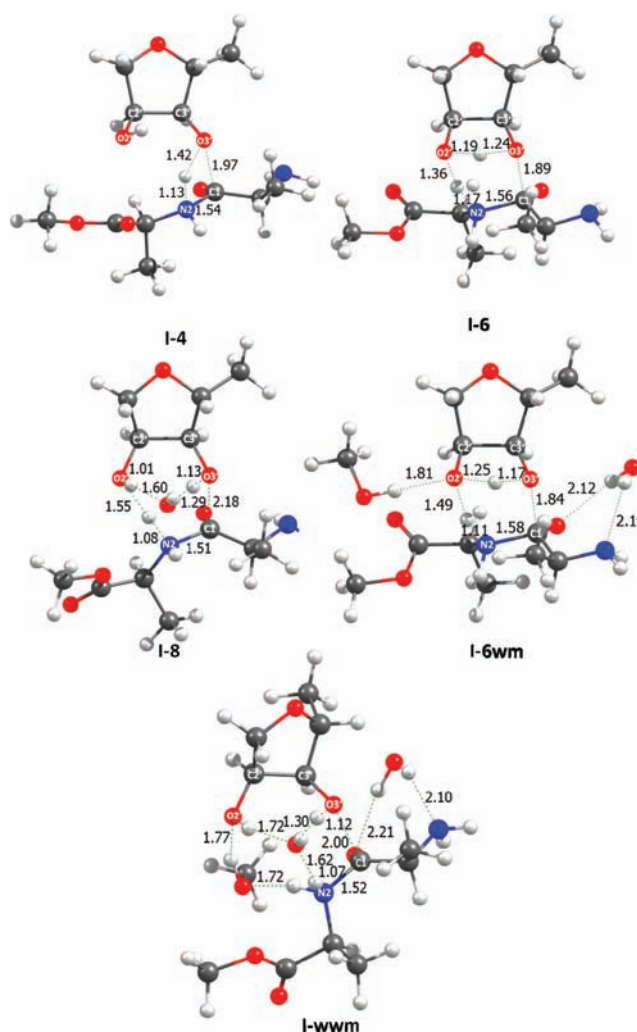


Figure 1. Transition structures for the five one-step mechanisms. Relevant distances in Å.

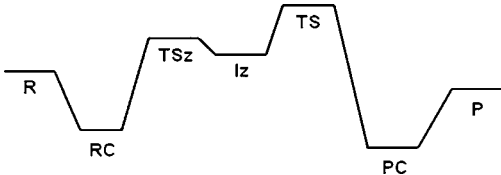
TS does not keep this eight-membered ring but, instead, two rings are formed. The formation of the first ring permits the activation of the O atom of the added water molecule as a proton donor through the formation of three hydrogen bonds between H2 and the O atom of the methanol molecule, between the H of methanol and the O2' of the sugar, and between H1' and the O atom of the added water molecule, which will transfer a proton to O3'. The two hydrogen bonds formed by the methanol molecule (which in our model represents the role of the 2'-OH of the A2451 nucleotide) help to correctly position the substrate as suggested by some authors and confirmed by X-ray data.^{12,29,34–37} So, the O2' atom does not play a direct role in the transfer of the H1 atom linked to N2 to O3', this transfer being done through the added water molecule in the six-membered ring. In contrast, in the TS of the I-6wm mechanism, the A2451 2'-OH...H–NH hydrogen bond is not formed, in good agreement with a too large distance in the crystal structure of the PTC with TS analogues.³⁹

The C1–O1 bond length is ~ 1.21 Å in all TSs. This value corresponds to a typical double bond, so that a zwitterionic mechanism, in which the C1–O1 bond would have a single-bond character, can be excluded, even in the case of mechanisms I-6wm and I-wwm, in which the presence of a water molecule could favor the formation of a zwitterion.

Table 2. Dipole Moment (μ , in D), Charge Transfer (CT, in au) between Initial Reactants, Relevant Natural Charges (q , in au), and, in Parentheses, Their Variation with Respect to the Reaction Complexes for the Transition States of One-Step Mechanisms

mechanism	μ	CT	q				
			N2	H1	O3'	O1	O
I-4	5.30	-0.45	-0.73 (0.13)	0.51 (0.14)	-0.84 (-0.22)	-0.67 (-0.04)	
I-6	6.57	-0.42	-0.73 (0.13)	0.49 (0.12)	-0.75 (-0.14)	-0.70 (-0.07)	
I-8	5.53	-0.52	-0.75 (0.12)	0.51 (0.13)	-0.83 (-0.20)	-0.61 (0.01)	-1.18 (-0.21)
I-6wm	7.61	-0.45	-0.72 (0.17)	0.49 (0.10)	-0.73 (-0.16)	-0.72 (-0.08)	
I-wwm	6.01	-0.49	-0.77 (0.13)	0.51 (0.13)	-0.80 (-0.19)	-0.68 (-0.05)	-1.16 (-0.20)

Table 3. Summary of Energies (kcal/mol) at the M06-2X/6-311+G(d,p) Level of Calculation for the Uncatalyzed I-4S and I-6S Reactions^a



mechanism	energy ^b	R	RC	TSz	Iz	TS	PC	P
I-4S	$\Delta E'$	0.0	-6.26 (-7.86)	6.21 (4.74)	5.61 (4.15)	24.63 (20.70)	-14.66 (-15.75)	-6.46 (-6.17)
	$\Delta H'$	0.0	-4.54	7.19	7.74	25.42	-13.23	-6.35
	ΔG	0.0	5.94	19.67	21.28	38.06	-2.52	-6.58
I-6S	$\Delta E'$	0.0	-5.18 (-6.52)			24.54 (21.01)	-15.05 (-16.74)	-6.55 (-6.02)
	$\Delta H'$	0.0	-3.18			24.70	-13.43	-6.33
	ΔG	0.0	7.79			37.68	-2.57	-5.76

^aValues in parentheses correspond to the MP2/6-311+G(d,p)//M06-2X/6-311+G(d,p) level of calculation. ^bThe values of E' are calculated by adding the terms of solvation free energy to the gas-phase PES. Thermodynamic corrections to obtain H' and G are computed in the modified surface.

This is confirmed by the Wiberg bond indexes,⁹¹ which are included in the Supporting Information, since their values for the C1–O1 bond in the TSs vary from 1.63 in the I-6wm mechanism to 1.78 in the I-8 mechanism, quite close to the values in the RC (~1.75). In contrast, the breaking of the C1–O3' bond and simultaneous formation of the N2–C1 bond imply a certain tetrahedral character of the geometry around C1. To confirm this, we computed the sum of the six bond angles around C1, this sum being expected to be 657° in an sp³ hybridization scheme and 630° when the sp² hybridization of the C1 atom is maintained while the attacking or leaving groups are far away. We observed that the sum of the six angles is ~630° in the RC and PC, while its ranges between 645° and 652° in the TS, the latter thus having a certain tetrahedral character. The sign of the C3'O3'C1N2 dihedral angle in the TS shows the side on which the attack is produced. In all the TSs, this dihedral is negative, corresponding to an S chirality as suggested by Schmeing et al.¹⁵ Finally, to discuss the proposal of Lang et al.³⁹ that was mentioned in the Introduction, the pseudorotation angle P was computed.⁹⁰ In the case of the mechanism I-6wm, in which the role of the A2451 nucleotide is modeled by a methanol molecule, one can observe that P increases regularly from R to P, in such a way that R corresponds to a C3' endo conformation and P to a C2' endo one.

Table 2 presents the dipole moments, the charge transfer from the nucleophile to the electrophile, the natural atomic populations over the N2, H1, O3', and O1 atoms, and the variation of these atomic populations with respect to the RCs for the TSs of the five studied mechanisms. In mechanisms I-8

and I-wwm, the O atom of the water molecule is also included. One can observe that the dipole moment of the TS is quite large in all cases, a fact which is related to the noticeable charge transfer between the two fragments. It is also worth mentioning that the N2 and H1 atoms lose electrons when passing from the RC to the TS, these electrons being mainly transferred to the O3' atom, favoring hydrogen bond transfer from N2 to O3'. In contrast, the natural population of the O1 atom barely changes. For mechanisms I-8 and I-wwm, the electron charge is also transferred to the O atom of the included water molecule, emphasizing the role played by this water molecule in the shuttle mechanism of the hydrogen transfer.

In Solution (Uncatalyzed Reaction). Table 3 is analogous to Table 1 for the two studied uncatalyzed mechanisms in solution. As a zwitterionic intermediate (Iz) appears in one of these mechanisms, this intermediate and the corresponding TS (TSz) are included in Table 3. The two mechanisms in Table 3 take into account the solvent effect of water using the SMD method.⁸⁵ The energy and enthalpy are indicated as E' and H' , since the computed energy is obtained by adding free energy of solvation to gas-phase potential energy surface (PES). This new E' surface is named, according to statistical mechanics, potential of mean force.⁹² In contrast, G is the real free energy as it contains the free energy of solvation.

The starting points for studying the two mechanisms in solution are the TS structures of the four- and six-membered ring mechanism in the ribosome (mechanisms I-4 and I-6). The two mechanisms in solution are called I-4S and I-6S, respectively, although the energy values of the RC, PC, and TS are quite similar

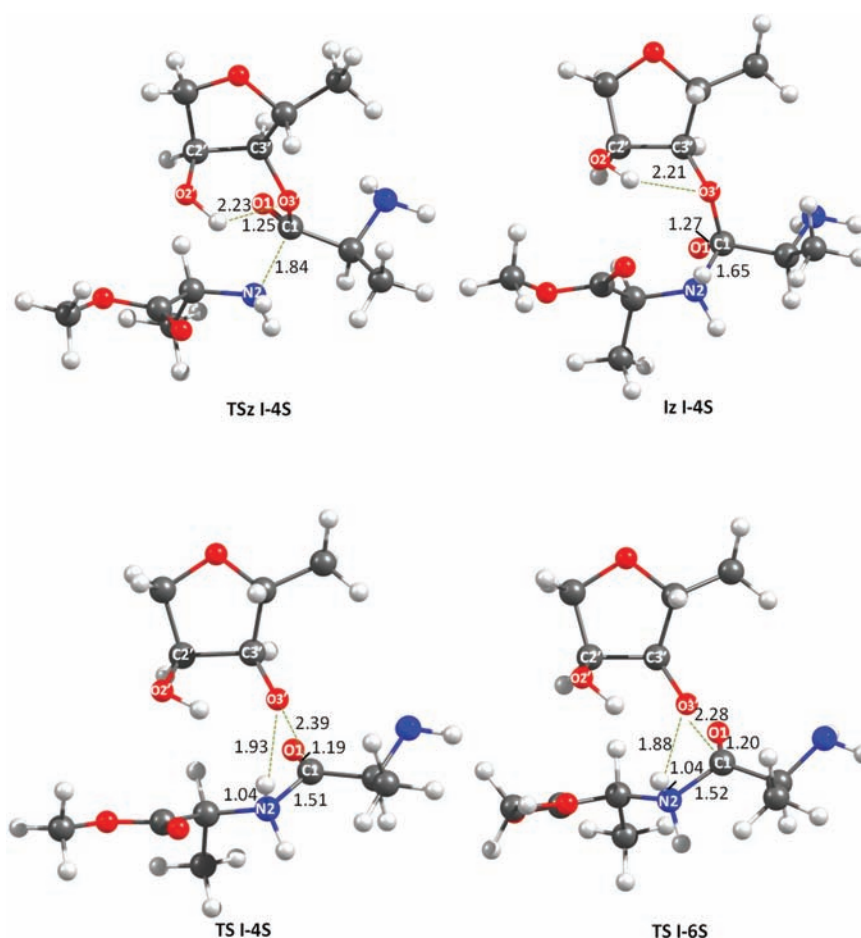


Figure 2. Transition and zwitterionic structures for the uncatalyzed one-step reactions. Relevant distances in Å.

Table 4. Dipole Moment (μ , in D), Charge Transfer (CT, in au) between Initial Reactants, Relevant Natural Charges (q , in au), and, in Parentheses, Their Variation with Respect to the Reaction Complexes for the Transition States and Zwitterion of One-Step Uncatalyzed Mechanisms

mechanism	μ	CT	q			
			N2	H1	O3'	O1
I-4S (TSz)	8.35	-0.36	-0.71 (0.17)	0.44 (0.06)	-0.68 (-0.11)	-0.86 (-0.17)
I-4S (Iz)	10.13	-0.50	-0.65 (0.23)	0.46 (0.08)	-0.70 (-0.13)	-0.93 (-0.24)
I-4S (TS)	15.47	-0.60	-0.68 (0.20)	0.52 (0.14)	-1.01 (-0.44)	-0.60 (0.09)
I-6S (TS)	15.26	-0.59	-0.69 (0.19)	0.52 (0.14)	-0.99 (-0.40)	-0.63 (0.05)

in both mechanisms, the main difference being the appearance of an Iz in the I-4S mechanism. The fact that the free energy of the RC is higher than that of the R had to be expected, as the solvent does not play the role of an entropy trap.

Figure 2 shows the geometries of the transition structures of both mechanisms and of the zwitterionic intermediate of mechanism I-4S. The dipole moments, the charge transfer from the nucleophile to the electrophile, the natural atomic populations over the N2, H1, O3', and O1 atoms, and the variation of these atomic populations with respect to the RCs for the TSs of the two studied mechanisms are presented in Table 4.

If one considers the I-4S (TS) and I-6S (TS) structures, one can observe that the N2-H1 hydrogen bond is only 0.02 Å longer than the value corresponding to R, while the C1-O3' is already notably broken. The hydrogen transfer is produced, in both mechanisms, through a four-membered ring cycle (as mentioned above, I-6S is named on the basis of the I-6 (TS) that we used as starting point for computing the TS in

solution). Analysis of the eigenvalues of the force constant matrix shows that it is a true TS since it has only one imaginary frequency ($\sim 200 \text{ cm}^{-1}$), and the transition vector corresponds to the transfer of the H1 atom from N1 to O3' and to the breaking of the C1-O3' bond. When comparing these TSs to the equivalent one in the ribosome (mechanism I-4 of Figure 1), one can observe that they are quite different, the hydrogen transfer being more advanced in the ribosome ($\text{O3}'\text{-H1} = 1.42 \text{ \AA}$) than in solution ($\text{O3}'\text{-H1} \approx 1.90 \text{ \AA}$).

The main difference between Tables 2 and 4 is the dramatic increase of the dipole moment in solution (uncatalyzed reaction), which is obviously related to the change of electron population in the O3' atom. Figure 2 shows that the TSs in solution can be considered as formed by two fragments since the distances C1-O3' (2.39 and 2.28 Å for I-4S and I-6S, respectively) and H1-O3' (1.93 and 1.88 Å) are quite long. The net charges over the sugar fragments are very large (-0.84 au for I-6S), in such a way that the TS has an ion-pair (IP)

character. To better understand this mechanism, one has to consider the effect of the polarization induced by the solvent reaction field. In fact, if one computes the dipole moment of I-6S (TS) *in vacuo* at the geometry optimized in solution (Figure 2), the dipole moment diminishes from 15.26 to 10.84 D, showing the great contribution of the polarization effect. Similar changes are found in the charge transfer and in the variation of the charges of the four atoms considered in Table 4. As has already been mentioned, the calculated energies shown in Table 3 for the mechanisms in solution were obtained by adding the free energy of solvation to the gas-phase PES. For the case of mechanism I-6S, it is possible to estimate the value of the activation free energy of solvation if one subtracts the E' value of 24.54 kcal/mol from the potential energy barrier of 36.17 kcal/mol, which was calculated *in vacuo* for the geometries optimized in solution. Thus, the free energy of solvation stabilizes the TS by 11.6 kcal/mol, as expected given the high value of the TS dipole moment. This stabilization comes, as usual, from the enthalpy and entropy terms. Given that the formation of an IP leads to a reorganization of the solvent, which will be associated with a decrease of entropy, the enthalpy term will be much greater than 11.6 kcal/mol. The solvent entropy destabilization of the TS was previously suggested by Warshel.⁵⁵

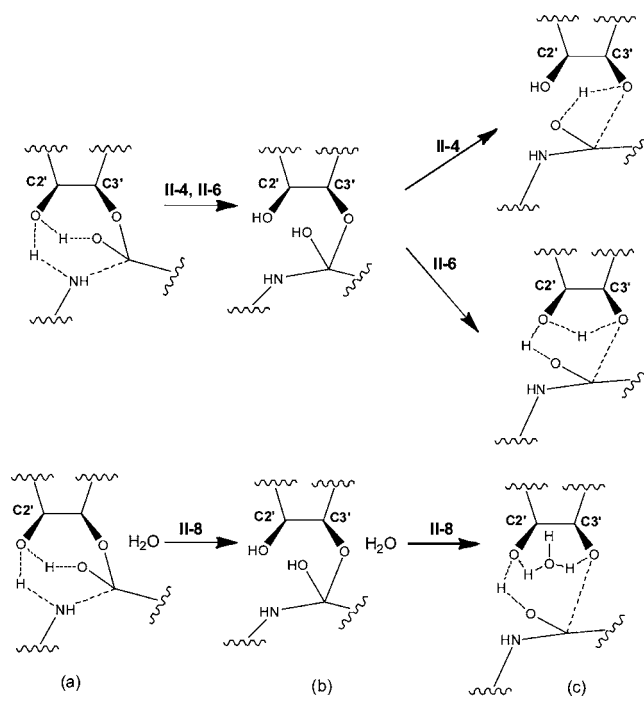
The most important difference between mechanisms I-4S and I-6S is the existence of an Iz in the first one. However, it is worth mentioning that the TSz is only 0.6 kcal/mol higher in energy than the intermediate, whereas the energy profile corresponding to the I-6S mechanism presents a sort of shoulder, with a very slight energy variation in this region of the IRC. To our knowledge, this is the first time that an Iz is found using a continuum model. Up to the present, this intermediate had only been located using a discrete representation of the solvent.^{93,94}

Let us now consider the zwitterionic stationary point structures (TSz and Iz). Figure 2 shows that both structures are close to the reactants, in such a way that the N2–C1 distances are still quite large (1.84 and 1.65 Å for TSz and Iz, respectively), while the C1–O1 bond lengths are 1.25 and 1.27 Å, respectively. Despite the small increase of the C1–O1 bond lengths, the Wiberg bond indexes (1.45 and 1.34) show that the double bond character has notably decreased. One can also observe in Table 4 that there is a large charge transfer from N2 to the O atoms, especially to the O1 one, in good agreement with what was expected for a zwitterionic structure.

Due to the presence of this Iz (T_{\pm} in the terminology of Strobel's group^{40,44}), mechanism I-4S involves two steps, although the intermediate is in a very shallow well. Strobel also proposes a three-step pathway for the uncatalyzed reaction, involving two tetrahedral intermediates (T_{\pm} and T^{-}), but, as he states, this mechanism is only possible at high pH, which is not the case studied in our work. As indicated above, the TS we found rather corresponds to an IP structure.

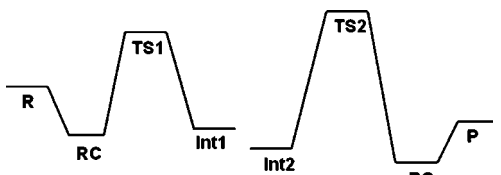
Two-Step Mechanisms. *In the Ribosome.* The three studied two-step mechanisms (II-4, II-6, and II-8) are those depicted in Scheme 5. It can be observed that the first steps of mechanisms II-4 and II-6 are the same, the TS being a six-membered ring in which the H1 atom is transferred from N2 to O2' while the H1' atom is transferred from O2' to O1. At the same time there is a nucleophilic attack of N2 to C1 to form the N2–C1 bond. The second steps of mechanisms II-4 and II-6 differ in the way the H atom linked to O1 is transferred to O3'. In mechanism II-4 the transfer is done directly through a four-membered cycle, while in mechanism II-6 the transfer is done through a six-membered cycle with the intervention of the 2'-OH.

Scheme 5. Schematic Representation of the Three Studied Two-Step Mechanisms, II-4, II-6, and II-8: (a) First Transition State, (b) Intermediate, and (c) Second Transition State



In the second step of mechanism II-8, the hydrogen transfer takes place through an eight-membered cycle in which a water molecule is incorporated. The first step is similar to those of mechanisms II-4 and II-6, although the six-membered cycle is slightly perturbed by the presence of the out-of-the-cycle water molecule.

Table 5 shows the variation, with respect to those of R, of the potential energy, the enthalpy, and the Gibbs free energy corresponding to the RC, transition states TS1 and TS2, the intermediates between the TSs, Int1 and Int2, the PC, and P for mechanisms II-4, II-6, and II-8. The optimizations were carried out using the M06-2X functional. For each stationary point, MP2//M06-2X calculations were also done. It can be observed that, in all cases, TS2 lies higher than TS1, both TSs having the lower energy in mechanism II-8. If one looks at the values corresponding to the P, one can observe that the enthalpy and the Gibbs free energy are very similar, implying a small value of the entropy term, as expected given the presence of two molecules in the R and P. In contrast, the entropy term is clearly positive in the complexes, TSs, and intermediates, since there is now one molecule instead of the two in the R. It is also worth mentioning that all the processes are exothermic, the values being very similar for one- and two-step mechanisms, especially if one compares I-6 and II-6 or I-8 and II-8. In fact, the small differences between these mechanisms can be attributed to slight differences in the conformations of the products obtained in each case. The presence of two intermediates (Int1 and Int2) in Table 5 is due to the methodology we used to obtain them. As indicated in the Computational Methods, the intermediates Int1 and Int2 were identified through the calculation of the IRC starting from TS1 and TS2, respectively. In fact, the two intermediates correspond to different conformers of the same chemical species. The energy difference between the two structures is quite small in mechanisms II-6 (−3.47 kcal/mol)

Table 5. Summary of Energies (kcal/mol) at the M06-2X/6-311+G(d,p) Level of Calculation for the Two-Step Mechanisms^a


mechanism	energy	R	RC	TS1	Int1	Int2	TS2	PC	P
II-4	ΔE	0.0	-8.27 (-9.44)	16.00 (12.93)	-5.83 (-4.90)	10.38 (12.15)	23.09 (23.11)	-20.43 (-21.39)	-4.67 (-5.65)
	ΔH	0.0	-6.81	13.66	-4.08	12.12	22.88	-18.76	-4.63
	ΔG	0.0	4.41	30.22	11.27	28.62	38.88	-5.38	-5.14
II-6	ΔE	0.0	-8.27 (-9.44)	16.00 (12.93)	-5.83 (-4.90)	-9.30 (-10.34)	24.77 (21.65)	-20.01 (-20.81)	-4.41 (-4.29)
	ΔH	0.0	-6.81	13.66	-4.08	-6.91	21.57	-18.40	-4.26
	ΔG	0.0	4.41	30.22	11.27	10.20	36.91	-5.79	-4.05
II-8	ΔE	0.0	-12.00 (-11.47)	7.60 (4.77)	-9.59 (-8.31)	-8.95 (-6.98)	13.86 (15.85)	-24.25 (-23.74)	-6.48 (-4.81)
	ΔH	0.0	-10.26	6.15	-7.69	-6.67	10.21	-22.56	-6.19
	ΔG	0.0	3.30	24.39	8.04	10.47	27.87	-8.18	-5.56

^aValues in parentheses correspond to the MP2/6-311+G(d,p)//M06-2X/6-311+G(d,p) level of calculation.

and II-8 (0.64 kcal/mol), but it is surprisingly high (16.21 kcal/mol) in mechanism II-4.

The geometries of the TSs of the three two-step mechanisms are shown in Figures 3 (mechanisms II-4 and II-6) and 5

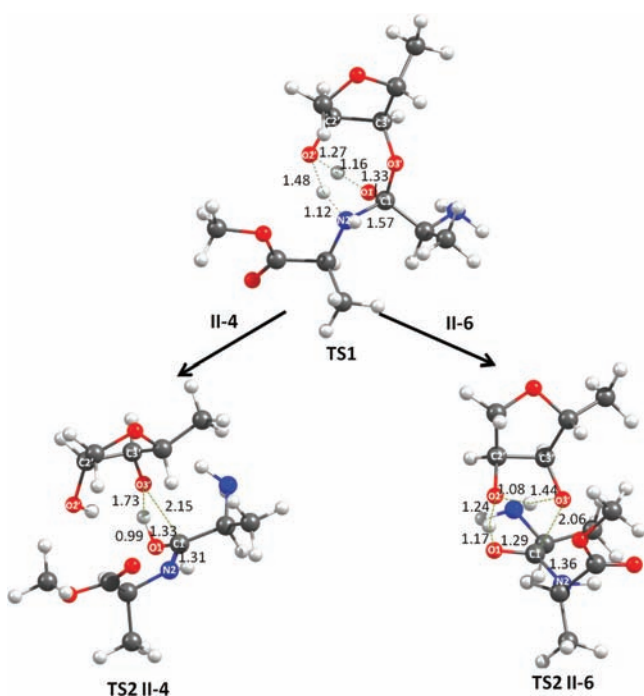


Figure 3. Transition state structures for the two-step mechanisms II-4 and II-6. Relevant distances in Å.

(mechanism II-8). Schematic representations of the intermediates are shown in Figures 4 (mechanisms II-4 and II-6) and 6 (mechanism II-8). Figure 3 shows that in the first TS (common to mechanisms II-4 and II-6) the hydrogen transfer from O2' to O1 is much more advanced than the one from N2

to O2'. It is also shown that the C1–O1 bond already has an important single-bond character (its bond length having increased from 1.21 Å in the RC to 1.33 Å in TS1, the corresponding Wiberg bond indexes being 1.73 and 1.11, respectively). The geometry around C1 is already quite tetrahedral, the sum of the six angles being close to 657°. In Int1 (Figure 4), both H atoms have already been transferred, accompanied by an increase of the degree of formation of the C1–N2 bond and an increase of the single-bond character of the C1–O1 bond (its Wiberg bond index is 0.96).

As has already been mentioned, the second step is different for mechanisms II-4 and II-6. This step corresponds to the hydrogen transfer from O1 to O3' and implies the breaking of the C1–O3' bond. If one compares the TS2 for mechanisms II-4 and II-6, one can observe that the hydrogen transfer is much more advanced in mechanism II-6 (the O1–H bond length is 1.17 Å) than in mechanism II-4 (O1–H = 0.99 Å). The more advanced hydrogen transfer in mechanism II-6 is accompanied by an increase of the double-bond character of the C1–O1 bond and a decrease in the degree of formation of the C1–N2 bond. The main difference between mechanisms II-4 and II-6 is that the C3'O3'C1N2 dihedral angle is negative in TS2 of mechanism II-6 (corresponding to an S chirality, as in the one-step mechanisms), while it is positive in TS2 of mechanism II-4 (this would lead to R chirality). All these differences between II-4 and II-6 TS2 structures imply that Int2 intermediates obtained for the two mechanisms will also differ (see, for instance, the bond lengths C1–N2, C1–O1, and C1–O3' in Figure 4). As in the TS2 structures, the Int2 intermediates of the two mechanisms have quite different conformations. The C3'O3'C1N2 dihedral angle, for instance, is negative for II-6 and positive for II-4. Moreover, the C2'C3'O3'C1 dihedral angle, which corresponds to the rotation around the C3'–O3' bond, differs by ~150° between the two mechanisms, leading to completely different conformers. Finally, if one compares Int1 with both Int2 intermediates, one can observe that the bond lengths in Int1 and Int2 are very similar in mechanism

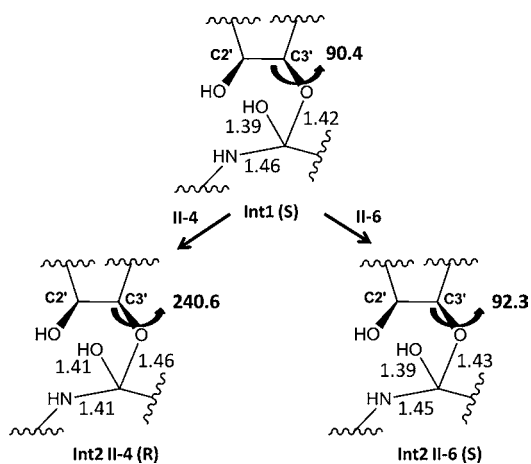


Figure 4. Schematic representation of the three intermediates of the II-4 and II-6 mechanisms. Relevant distances in Å, and C2'C3'O3'C1 dihedral angle in degrees.

II-6, but that important changes exist for mechanism II-4. Similar conclusions can be obtained from the C3'O3'C1N2 and C2'C3'O3'C1 dihedral angles. These results seem to indicate that mechanism II-4 can be disregarded, since it is unlikely that such important conformational changes could take place in the active center of ribosome.

Let us now consider mechanism II-8 (Figures 5 and 6). The first step is very similar to that of mechanisms II-4 and II-6,

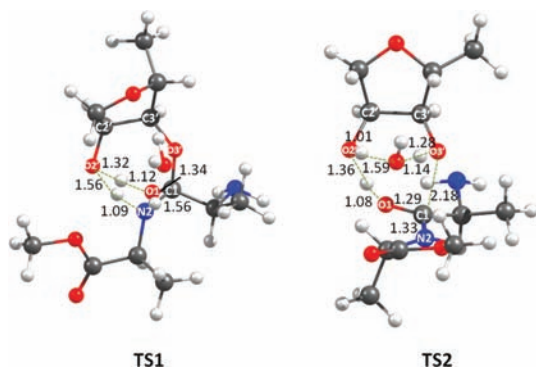


Figure 5. Transition state structures for the two-step mechanism II-8. Relevant distances in Å.

since the inclusion of a water molecule provokes only a slight perturbation of TS1 and Int1 structures. Regarding the second step, one can observe that the TS2 structure is similar to the one of mechanism II-6, the main difference being that the O1–H bond is less broken while the formation of the O3'–H bond is more advanced in mechanism II-8 than in mechanism II-6. Similar conclusions can be obtained from the tetrahedral character of the C1 atom, from the negative value of the C3'O3'C1N2 dihedral angle, and from the similar values of the C2'C3'O3'C1 dihedral angles. As in the case of mechanism II-6, Int1 and Int2 of mechanism II-8 are also very similar, both presenting a tetrahedral character with S chirality (see Figure 6).

Table 6 presents the dipole moments, the natural atomic populations over the N2, H1, O3', and O1 atoms, and the variation of these atomic populations with respect to the RCs for the TSs and Int1 of the three studied mechanisms. For mechanism II-8, the natural atomic population of the O atom of the water molecule is also included. One can observe that the

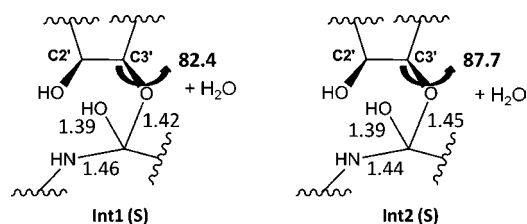


Figure 6. Schematic representation of the two intermediates of the II-8 mechanism. Relevant distances in Å, and C2'C3'O3'C1 dihedral angle in degrees.

charges over the N2 and H1 atoms of the first TS become less negative and more positive, respectively, and that the negative charge increases, especially over the O1 atom, in such a way that the TS1 structures have a zwitterionic character. This zwitterionic character is a bit less important in the Int1 intermediates, since the electronic transfer to the O1 atom is smaller in them, in good agreement with the lower value of the dipole moment of the intermediates. The presence of a zwitterionic TS is in good agreement with the experimental results of Schmeing et al.¹⁵ In the second step, the N2 atom continues to lose electronic charge, but now it is the O3' atom (and also the O atom of the water molecule in mechanism II-8) that becomes more negative. As this electronic transfer is accompanied by the breaking of the C1–O3' bond, the TS2 structures have now an IP character, in a similar way to what happened for the TSs of the one-step mechanisms.

In Solution (Uncatalyzed Reaction). Table 7 is analogous to Table 5 for the two studied uncatalyzed mechanisms in solution. The starting points for studying the two mechanisms are the TSs of the four- and six-membered ring mechanisms in the ribosome (mechanisms II-4 and II-6). These two mechanisms are called II-4S and II-6S, respectively. An Iz appears in the first step of both mechanisms. This intermediate and the corresponding TSz are included in Table 7.

One can observe that the well of the Iz is deeper in the two-step than in the one-step mechanism, the energy difference between TSz and Iz being now 1.31 kcal/mol instead of 0.60 kcal/mol in the I-4S mechanism. The second main difference between Tables 5 and 7 is that the IRC from TS2 does not lead to the PC, as was the case in the two-step mechanism in the ribosome, but to an IP.

Figure 7 shows the geometries of the four TSs of II-4S and II-6S mechanisms, while the geometries of the Iz and of the two IPs are presented in Figure 8. Dipole moments (μ), relevant natural charges (q), and their variation with respect to the RCs for the TSs and intermediates of the two-step mechanisms in solution are presented in Table 8.

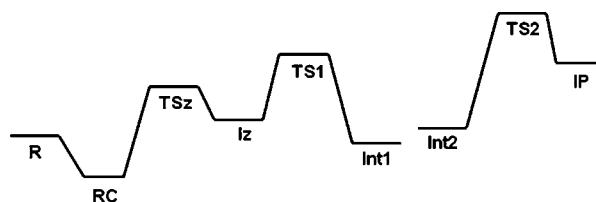
As in the case of the uncatalyzed one-step mechanism, Figures 7 and 8 show that TSz and Iz are close to reactants, since the N2–C1 distances are still quite large (1.92 and 1.63 Å for TSz and Iz, respectively), while the C1–O1 bond lengths are 1.25 and 1.29 Å, respectively. Despite the small increase of the C1–O1 bond lengths, the Wiberg bond indexes (1.44 and 1.26) show that the double bond character has notably decreased. One can also observe in Table 8 that there is a large charge transfer from N2 to the O atoms, especially to O1, as expected for a zwitterionic structure.

When one compares Tables 6 and 8, one can observe that the dipole moments of TSs are much larger in solution than in the ribosome. This is related to the fact that in TS2 the hydrogen transfer from O1 to O3' is less advanced when it is direct (mechanism II-4S) than when the transfer occurs through the

Table 6. Dipole Moment (μ , in D), Relevant Natural Charges (q , in au), and, in Parentheses, Their Variation with Respect to the Reactant Complexes for the Transition States and Intermediates of the Two-Step Mechanisms

stationary point	μ	q				
		N2	H1	O3'	O1	O
TS1 II-4, II-6	4.63	-0.71 (0.15)	0.50 (0.12)	-0.67 (-0.09)	-0.83 (-0.19)	
Int1 II-4, II-6	2.61	-0.75 (0.11)	0.49 (0.11)	-0.66 (-0.08)	-0.78 (-0.14)	
TS2 II-4	5.14	-0.61 (0.25)	0.48 (0.10)	-0.96 (-0.38)	-0.75 (-0.11)	
TS2 II-6	2.50	-0.65 (0.21)	0.52 (0.14)	-0.85 (-0.27)	-0.79 (-0.15)	
TS1 II-8	3.54	-0.75 (0.15)	0.50 (0.11)	-0.67 (-0.08)	-0.82 (-0.16)	-0.98 (-0.01)
Int1 II-8	2.26	-0.78 (0.12)	0.50 (0.11)	-0.68 (-0.09)	-0.78 (-0.12)	-0.97 (0.00)
TS2 II-8	5.02	-0.64 (0.26)	0.52 (0.13)	-0.87 (-0.28)	-0.75 (-0.09)	-1.09 (-0.12)

Table 7. Summary of Energies (kcal/mol) at the M06-2X/6-311+G(d,p) Level of Calculation for the II-4S and II-6S Mechanisms^a



mechanism	energy ^b	R	RC	TSz	Iz	TS1	Int1	Int2	TS2	IP
II-4S	$\Delta E'$	0.0	-7.10 (-8.20)	7.03 (6.62)	5.72 (4.26)	13.33 (10.21)	-0.16 (-1.04)	0.83 (-0.35)	21.93 (20.91)	17.18 (16.20)
	$\Delta H'$	0.0	-5.90	7.91	7.71	13.19	1.74	3.26	22.33	17.59
	ΔG	0.0	4.61	21.60	21.42	28.70	15.51	18.08	35.95	29.22
II-6S	$\Delta E'$	0.0	-7.10 (-8.20)	7.03 (6.62)	5.72 (4.26)	13.33 (10.21)	-0.16 (-1.04)	-6.04 (-7.49)	22.86 (22.14)	19.32 (19.41)
	$\Delta H'$	0.0	-5.90	7.91	7.71	13.19	1.74	-3.70	22.72	19.02
	ΔG	0.0	4.61	21.60	21.42	28.70	15.51	11.75	37.44	29.18

^aValues in parentheses correspond to the MP2/6-311+G(d,p)//M06-2X/6-311+G(d,p) level of calculation. ^bThe values of E' are calculated by adding the terms of solvation free energy to the gas-phase PES. Thermodynamic corrections to obtain H' and G are computed in the modified surface.

O2'-H (mechanism II-6S). Analysis of the components of the transition vector shows that hydrogen transfer does not participate in the reaction coordinate, which corresponds mainly to the heterolytic breaking of the C1-O3' bond, leading to the formation of an IP. Regarding TS1, the increase of the dipole moment is due to the fact that hydrogen transfer from O2' to O1 is more advanced in solution than in the ribosome, while the opposite is true for the transfer from the N2 to O2' (see Figures 3 and 7).

Let us now consider the IPs found in mechanisms II-4S and II-6S. Figure 8 shows the existence of two fragments as a consequence of the heterolytic breaking of the C1-O3' (the distance between these two atoms being 2.90 and 3.37 Å for II-4S and II-6S, respectively). However, in both cases a hydrogen bond is formed between the two fragments, the O1-H...O2' hydrogen bond in the II-6S mechanism being stronger than the other one. As expected, Table 8 shows that the dipole moments of these two species are very large. These values can be mainly attributed to the charge transfer from the N2 atom to the O3' atom. The IP character is confirmed by the charge over the two fragments, which is 0.96 for II-4S and 0.87 for II-6S.

Finally, schematic representations of the Int1 and Int2 intermediates can be found in the Supporting Information, since the comments on these stationary points would be very similar to those corresponding to the equivalent intermediates of the two-step mechanisms in ribosome (Figure 4).

DISCUSSION AND CONCLUSIONS

As stated above, two different kinds of mechanisms have been considered. In the one-step mechanisms, nucleophilic attack of the N atom to the carboxylic C atom is accompanied by the transfer of a H atom to the C-O oxygen atom of the carboxylic group. For the two-step mechanisms, the H atom is first transferred to the C=O oxygen atom of the carboxylic group, and, in a second step, the transfer to the other O atom is produced. In the latter mechanism it is found (see Table 5) that the highest energy transition structure is the one corresponding to the second step (TS2) and that the TS1 and the intermediate have some zwitterionic character. If one compares the TS2 with the transition structures of the one-step mechanisms, one can observe that, in both cases, the heterolytic breaking of the C1-O3' bond is quite advanced, while the hydrogen transfer is only at an initial stage, such that the two transition structures have some IP character. Despite this similarity, comparison of Figures 1, 3, and 5 shows that the C1-O1 bond has a greater single-bond character and that the C1-N2 bond is more formed in TS2 than in TS. It is worth mentioning that the Iz suggested by some authors (see Scheme 1) has never been found for the reaction in the ribosome, neither in the computed IRCs nor when appropriate regions of the PES have been explored. In contrast, an Iz does appear at the beginning of the process when the uncatalyzed reactions in solution is considered. These intermediates are not relevant

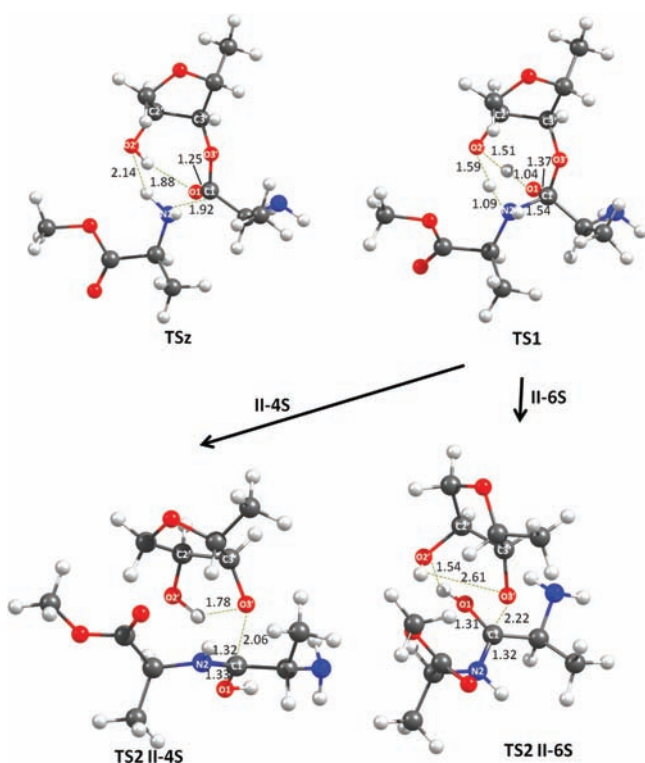


Figure 7. Transition state structures for the two-step mechanisms II-4S and II-6S. Relevant distances in Å.

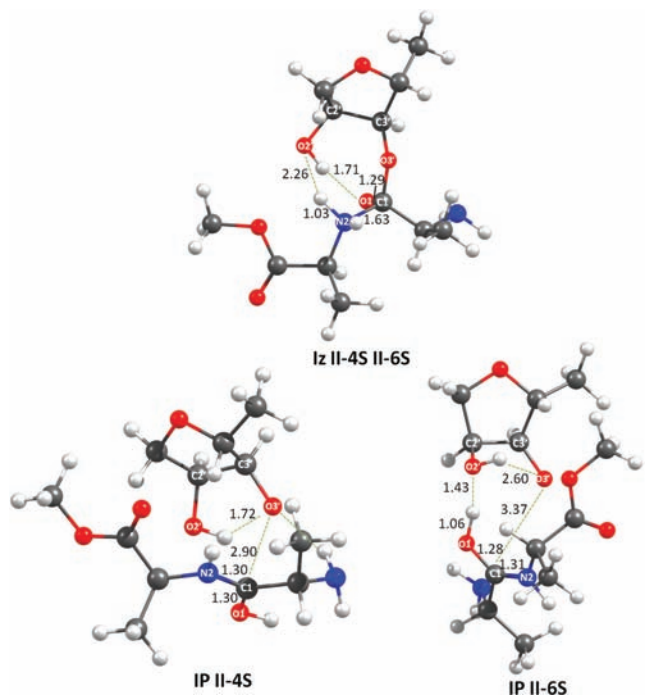


Figure 8. Structures of the zwitterionic and ion-pair intermediates of the II-4S and II-6S mechanisms. Relevant distances in Å.

from a kinetic point of view, since the rate-limiting step is the heterolytic breaking of the C1–O3' bond, which is accompanied by the transfer of one proton to O3', this proton coming from N2 in the one-step mechanism and from O1 in the two-step one. It is also interesting to emphasize that one important effect of the solvent is to affect the relative extent of bond

breaking and bond formation, such that the C–O bond dissociation, for instance, is much more advanced in solution, while the proton transfer from N2 to O3' is noticeably delayed.

The TSs of the four-membered ring mechanisms (I-4 and II-4) computed in this paper at the M06-2X level of calculation (Tables 1 and 5) are slightly lower in energy than those previously found by Yonath's group^{62,63} and Wang et al.,⁶⁶ both computed at the B3LYP level, for mechanisms I-4 and II-4, respectively. Our results for mechanism I-6 (Table 1) are also slightly lower than the B3LYP ones of Wallin et al.⁶⁵ This shuttle mechanism was expected to be more favorable than mechanism I-4.^{15,30} However, the results in Table 1 show that this is not the case, mechanism I-4 having a smaller energy barrier. This has also been found by Thirumoorthy et al.⁶⁴ at the HF/3-21G level of calculation. To our knowledge, the two-step six-membered ring mechanism, II-6, has never been studied by other authors. In this work, it was found that this shuttle mechanism is again less favorable than the II-4 one. In contrast, the introduction of one water molecule in I-6 and II-6 mechanisms, which allows the formation of eight-membered ring structures (mechanisms I-8 and II-8), leads to a dramatic diminution of the energy barriers. This can be attributed to the fact that the water molecule increases the flexibility of the system. The role of bound water in catalytic actions was recently emphasized by Ball.⁹⁵ For mechanism I-6 (Table 1), it was also found that the introduction of one methanol molecule (modeling the 2'-OH group of A2451) and one water molecule, with the aim of stabilizing the Iz, lowers the energy barrier by ~5 kcal/mol. Nevertheless, this lowering of the energy barrier is not associated with the stabilization of the zwitterionic structure, as the C1–O1 bond keeps its double-bond character. Given that mechanism I-8 is clearly more favorable than mechanism I-6, we decided to investigate the effect of introducing one methanol molecule and one water molecule. This leads to mechanism I-wwm which, again, presents a dramatic lowering of the energy barrier, such that it becomes the most favorable one-step mechanism. It has to be emphasized that the nature of I-wwm mechanism is different from the other ones and has never been considered before. In this case, the transfer of the H atom from N1 to O3' is done through a water molecule without the intervention of 2'-OH, this hydroxyl having now the mission of anchoring the reactants and activating the water molecule which is acting in the hydrogen transfer.

The main goal of this theoretical work was to get a deeper insight into the mechanism of peptide bond formation in the ribosome. However, one has to be conscious of the methodological limitations which are inherent in QM studies of complex systems. The first limitation is due to the need to use a reduced model of the real system. At the same time, the effect of environment in the chemical processes is not introduced. This implies that the system is allowed to be more flexible than it really is, since the constraints due to the physical environment are not taken into account. Moreover, the electrostatic embedding, due to the electrical field created by the enzyme, is also not considered, whereas it is well known that the changes of the pK_a 's of ionizable groups in enzymes are directly related to the electrostatic field.⁹⁶ In particular, it was recently emphasized that charge states of the nucleobases of RNA enzymes make important catalytic contributions to ribozyme activity.⁹⁷

Despite these unavoidable limitations, QM studies permit us to get a better understanding of experimental results. The study of several structures which are analogues to the TS led Steitz^{14,15} to conclude that the mechanism of peptide synthesis in the ribosome

Table 8. Dipole Moments (μ , in D), Relevant Natural Charges (q , in au), and, in Parentheses, Their Variation with Respect to the Reactant Complexes for the Transition States and Intermediates of the Two-Step Mechanisms in Solution

stationary point	μ	q			
		N2	H1	O3'	O1
TSz II-4S, II-6S	3.85	-0.75 (0.14)	0.44 (0.06)	-0.67 (-0.08)	-0.85 (-0.17)
Iz II-4S, II-6S	6.58	-0.66 (0.23)	0.47 (0.09)	-0.69 (-0.10)	-0.94 (-0.26)
TS1 II-4S, II-6S	8.76	-0.70 (0.19)	0.50 (0.12)	-0.67 (-0.08)	-0.83 (-0.15)
Int1 II-4S, II-6S	2.93	-0.77 (0.12)	0.52 (0.14)	-0.67 (-0.08)	-0.79 (-0.11)
TS2 II-4S	7.83	-0.64 (0.25)	0.51 (0.13)	-0.94 (-0.35)	-0.71 (-0.03)
TS2 II-6S	8.91	-0.61 (0.28)	0.52 (0.14)	-0.99 (-0.40)	-0.75 (-0.07)
IP II-4S	13.07	-0.57 (0.32)	0.51 (0.13)	-1.06 (-0.47)	-0.65 (0.03)
IP II-6S	14.66	-0.56 (0.33)	0.52 (0.14)	-1.09 (-0.50)	-0.69 (-0.01)

goes through zwitterionic tetrahedral stationary points. Our results question this conclusion. In fact, the transition structures of the one-step mechanisms have some tetrahedral character, but they are rather IPs than zwitterions. In the case of the two-step mechanisms, it is true that the first TS has both tetrahedral and zwitterionic character, but, as shown in Table 5, the highest energy barrier corresponds to the second TS, this one presenting again an IP character. So, the structure of analogues does not always allow researchers to reach definite conclusions since, as recently stated, it is important to take into account both the geometry similarity and the charge balance.⁹⁸ Schmeing et al.¹⁵ suggested the participation of a second crystallographic water molecule linked to A2602 and U2584 as an oxyanion hole in a zwitterionic structure. However, a very recent paper¹⁶ argues from experimental data that the stabilization of the transition structure due to the water molecule is quite small. In fact, this zwitterionic structure was not identified in our work, seeming to confirm that the second water molecule is playing a minor role. Two experimental techniques also question the existence of an Iz if the process takes place in the ribosome. The first considers the slope of Brønsted linear free energy relationships, which is close to zero in the ribosome and close to one in solution.^{40,41} The second technique is the measurement of the kinetic isotope effect (KIE) on the N2 atom, which is normal in the ribosome, while it is inverse in ester aminolysis reactions in solution.^{42,44} Both techniques suggest that the nitrogen deprotonation occurs simultaneously with the formation of the C–N bond. Our results give theoretical support to this experimental interpretation.

A second point to be discussed is the role played by the proton shuttle mechanism. As mentioned in the Introduction, Weinger et al.³⁰ reported experimental evidence that this shuttle mechanism has an important participation in the catalytic process. Their opinion was supported by the works of other authors.^{15,24–29} However, the proton shuttle mechanism was questioned by Sprinzl.^{31,32} In a more recent paper, Green and Strobel's group³³ found that the kinetic contribution of the 2'-OH group to the catalysis is significantly smaller than they had previously obtained.³⁰ These new findings reconcile the conflict in the literature and support a model where interactions between active site residues and the 2'-OH are pivotal in orienting substrates in the active site for optimal catalysis. Our theoretical calculations clearly confirm these recent experimental works. As shown in Tables 1 and 3, the proton shuttle is not efficient in the six-membered ring mechanism, probably due to the rigidity of the sugar fragment. As previously stated by Steitz,¹⁵ our work shows that the presence of a crystallographic water molecule, linked to A2451 and other ligands of ribosome, makes the shuttle mechanism efficient through the formation of an eight-membered ring cycle. A very

recent paper on solvent isotope effects and proton inventories concludes that the rate-limiting step is the formation of three hydrogen bonds with about equal contributions, consistent with our scenario of a concerted eight-membered proton shuttle in the TS.⁴⁵ It would be interesting to do a similar study on the uncatalyzed reaction, since this would allow us to conclude on the possible intervention of water molecules on the proton transfer process. Some experimental studies^{34–39} also suggested that the 2'-OH group of A2451 plays an important role in the shuttle process. This fact was interpreted³⁹ through the induction of a best-adapted conformation of the sugar. Our work confirms this interpretation, but it also suggests that this 2'-OH group activates the proton donor character of the 2'-OH of A76 (mechanism I6-wm). Besides, in the proposed mechanism I-wwm, it has been shown that proton shuttling can also take place via a water molecule, which is activated by a chain process with intervention of both 2'-OH. This gives theoretical support to the recently proposed³³ pivotal intervention of the 2'-OH group.

A final point deserves to be discussed. Through the observation of isotope effects,^{42–44} the small slope of the Brønsted linear free energy relationships,^{40,41} and several kinetic studies,^{46–51} it has been shown that the mechanisms are very different in the ribosome and in solution. In particular, Hiller et al.⁴⁴ analyzed the KIE at five positions and concluded that, in contrast to the uncatalyzed reaction,⁴³ both the formation of the tetrahedral intermediate and the proton transfer from the nucleophilic nitrogen occur in the rate-limiting step. Given that the KIE at O1 has not been determined in the ribosome, let us consider the effect at O3' which is 1.029 in the uncatalyzed reaction and 1.006 in the reaction catalyzed by the ribosome. From these two values they conclude that the C–O bond dissociation is advanced in solution, while it is not significant in the ribosome. Our results show that the C–O bond dissociation is much more advanced in solution, but they also show that it is not negligible in the ribosome (see the geometries of TS in Figure 1 and of TS2 in Figures 3 and 5). The reason is that there is another factor that has to be taken into account to interpret the KIE values: the formation of the O3'-H bond, which, in contrast, is more advanced in the ribosome. The driving force for the formation of the O3'-H bond is that the heterolytic breaking of the C–O bond increases the basicity of O3' and the acidity of N2, this driving force being diminished by the solvent reaction field. It is also worth mentioning that our calculations indicate that the one-step mechanisms in solution (I-4S and I-6S) present, indeed, a high increase of the dipole moment (see Table 4), which can be in part attributed to reaction field polarization effects. In fact, the reaction in solution can be assimilated to an S_N2 process between two neutral molecules, which is similar to the Mentschutkin reaction, although, in our case,

the final products will also be neutral since a proton will be transferred from one fragment to the other. Furthermore, the high dipole moment of the TS will lead to an important reorganization of the solvent, which will imply a diminution of entropy, in good agreement with the increase of the entropy term ($-T\Delta S$) proposed by Sharma et al.⁴⁹

However, as we previously mentioned, the simplified model used in our calculations does not take into account the real role played by the ribosome as an entropy trap (orienting and positioning substrates), this fact leading to a positive value of the ΔG of formation of the RC. The introduction of the surrounding effects (mechanical and electrical embedding) played by the ribosome would need hybrid QM/MM calculations, but this is quite difficult for our system. On one side, the MM methodology is not yet well developed for RNA systems.^{99–101} Furthermore, the calculation of free energy surfaces would require a semiempirical method able to accurately reproduce the *ab initio* results obtained in this work. Another difficulty is that one would have to know, from solvent isotope effects,⁴⁵ if it is necessary to introduce water molecules in the QM subsystem for the study of peptide bond formation in solution. At present, this is beyond the scope of this work.

Despite the simplified model used in this paper, it permits us to advance in the understanding of the unsolved puzzle of the mechanism of peptide synthesis in the ribosome. Three main points suggested in this work deserve to be deeply analyzed. First, a zwitterionic transition structure is identified in two-step mechanisms, but no zwitterionic intermediates are found when the reaction takes place in the ribosome. Second, the proton shuttle mechanism is suggested to be efficient only through the participation of the A2451 2'-OH and two crystallographic water molecules. Finally, the mechanisms in solution and in ribosome are very different, this difference helping to understand the reason that is at the origin of the efficient catalytic role played by the ribosome.

■ ASSOCIATED CONTENT

■ Supporting Information

Complete ref 88; geometrical parameters of the transition structures; absolute energies (in Hartree) for all the optimized structures; Wiberg indexes of the C1–O1 bond of several structures; and a schematic representation of the Int1 and Int2 intermediates for II-4S and II-6S mechanisms. This material is available free of charge via the Internet at <http://pubs.acs.org>.

■ AUTHOR INFORMATION

■ Corresponding Author

bertran@klingon.uab.cat

■ Notes

The authors declare no competing financial interest.

■ ACKNOWLEDGMENTS

This paper is dedicated to Prof. Joseph J. Dannenberg (Hunter College, City University of New York) on the occasion of his 70th birthday. Financial support from Ministerio de Ciencia e Innovación (through Grants CTQ2008-06381 and CTQ2010-15408) and Generalitat de Catalunya (through the Grant SGR2009-733) and allowance of computer resources from the CIESCA supercomputing center are gratefully acknowledged.

■ REFERENCES

(1) Yonath, A. *Angew. Chem., Int. Ed.* **2010**, *49*, 4341.

- (2) Ramakrishnan, V. *Angew. Chem., Int. Ed.* **2010**, *49*, 4367.
(3) Steitz, T. A. *Angew. Chem., Int. Ed.* **2010**, *49*, 4388.
(4) Ban, N.; Nissen, P.; Hansen, J.; Moore, P. B.; Steitz, T. A. *Science* **2000**, *289*, 905.
(5) Schluenzen, F.; Tocilj, A.; Zarivach, R.; Harms, J.; Gluehmann, M.; Janell, D.; Bashan, A.; Bartels, H.; Agmon, I.; Franceschi, F.; Yonath, A. *Cell* **2000**, *102*, 615.
(6) Wimberly, B. T.; Brodersen, D. E.; Clemons, W. M.; Morgan-Warren, R. J.; Carter, A. P.; Vornrhein, C.; Hartsch, T.; Ramakrishnan, V. *Nature* **2000**, *407*, 327.
(7) Yusupov, M. M.; Yusupova, G. Z.; Baucom, A.; Lieberman, K.; Earnest, T. N.; Cate, J. H.; Noller, H. F. *Science* **2001**, *292*, 883.
(8) Nissen, P.; Hansen, J.; Ban, N.; Moore, P. B.; Steitz, T. A. *Science* **2000**, *289*, 920.
(9) Cech, T. R. *Science* **2000**, *289*, 878.
(10) Beringer, M.; Rodnina, M. V. *Mol. Cell* **2007**, *26*, 311.
(11) Beringer, M. *RNA* **2008**, *14*, 795.
(12) Hansen, J. L.; Schmeing, T. M.; Moore, P. B.; Steitz, T. A. *Proc. Natl. Acad. Sci. U.S.A.* **2002**, *99*, 11670.
(13) Welch, M.; Chastang, J.; Yarus, M. *Biochemistry* **1995**, *34*, 385.
(14) Steitz, T. A. *Nature Rev.* **2008**, *9*, 242.
(15) Schmeing, T. M.; Huang, K. S.; Kitchen, D. E.; Strobel, S. A.; Steitz, T. A. *Mol. Cell* **2005**, *20*, 437.
(16) Carrasco, N.; Hiller, D. A.; Strobel, S. A. *Biochemistry* **2011**, *50*, 10491.
(17) Muth, G. W.; Ortoleva-Donnelly, L.; Strobel, S. A. *Science* **2000**, *289*, 947.
(18) Tamura, K.; Schimmel, P. *Proc. Natl. Acad. Sci. U.S.A.* **2001**, *98*, 1393.
(19) Schmeing, T. M.; Seila, A. C.; Hansen, J. L.; Freeborn, B.; Soukup, J. K.; Scaringe, S. A.; Strobel, S. A.; Moore, P. B.; Steitz, T. A. *Nat. Struct. Biol.* **2002**, *9*, 225.
(20) Katunin, V. I.; Muth, G. W.; Strobel, S. A.; Wintermeyer, W.; Rodnina, M. V. *Mol. Cell* **2002**, *10*, 339.
(21) Bieling, P.; Beringer, M.; Adio, S.; Rodnina, M. V. *Nat. Struct. Mol. Biol.* **2006**, *13*, 423.
(22) Polacek, N.; Gaynor, M.; Yassin, A.; Mankin, A. S. *Nature* **2001**, *411*, 498.
(23) Youngman, E. M.; Brunelle, J. L.; Kochaniak, A. B.; Green, R. *Cell* **2004**, *117*, 589.
(24) Dorner, S.; Polacek, N.; Schulmeister, U.; Panuschka, C.; Barta, A. *Biochem. Soc. Trans.* **2002**, *30*, 1131.
(25) Dorner, S.; Panuschka, C.; Schmid, W.; Barta, A. *Nucleic Acids Res.* **2003**, *31*, 6536.
(26) Steitz, T. A.; Moore, P. B. *Trends Biochem. Sci.* **2003**, *28*, 411.
(27) Moore, P. B.; Steitz, T. A. *RNA* **2003**, *9*, 155.
(28) Wohlgenuth, I.; Beringer, M.; Rodnina, M. V. *EMBO Rep.* **2006**, *7*, 699.
(29) Voorhees, R. M.; Weixlbaumer, A.; Loakes, D.; Kelley, A. C.; Ramakrishnan, V. *Nat. Struct. Mol. Biol.* **2009**, *16*, 528.
(30) Weinger, J. S.; Parnell, K. M.; Dorner, S.; Green, R.; Strobel, S. A. *Nat. Struct. Mol. Biol.* **2004**, *11*, 1101.
(31) Koch, M.; Huang, Y.; Sprinzl, M. *Angew. Chem., Int. Ed.* **2008**, *47*, 7242.
(32) Huang, Y.; Sprinzl, M. *Angew. Chem., Int. Ed.* **2011**, *50*, 7287.
(33) Zaher, H. S.; Shaw, J. J.; Strobel, S. A.; Green, R. *EMBO J.* **2011**, *30*, 2445.
(34) Erlacher, M. D.; Lang, K.; Shankaran, N.; Wotzel, B.; Hüttenhofer, A.; Micura, R.; Mankin, A. S.; Polacek, N. *Nucleic Acids Res.* **2005**, *33*, 1618.
(35) Erlacher, M. D.; Lang, K.; Wotzel, B.; Rieder, R.; Micura, R.; Polacek, N. *J. Am. Chem. Soc.* **2006**, *128*, 4453.
(36) Pech, M.; Nierhaus, K. H. *Chem. Biol.* **2008**, *15*, 417.
(37) Khade, P.; Joseph, S. *FEBS Lett.* **2010**, *584*, 420.
(38) Chirkova, A.; Erlacher, M.; Micura, R.; Polacek, N. *Curr. Org. Chem.* **2010**, *14*, 148.
(39) Lang, K.; Erlacher, M.; Wilson, D. N.; Micura, R.; Polacek, N. *Chem. Biol.* **2008**, *15*, 485.

- (40) Kingery, D. A.; Pfund, E.; Voorthees, R. M.; Okuda, K.; Wohlgemuth, I.; Kitchen, D. E.; Rodnina, M. V.; Strobel, S. A. *Chem. Biol.* **2008**, *15*, 493.
- (41) Kingery, D. A.; Strobel, S. A. *Acc. Chem. Res.* **2012**, DOI: 10.1021/ar100162b.
- (42) Seila, A. C.; Okuda, K.; Núñez, S.; Seila, A. F.; Strobel, S. A. *Biochemistry* **2005**, *44*, 4018.
- (43) Hiller, D. A.; Zhong, M.; Singh, V.; Strobel, S. A. *Biochemistry* **2010**, *49*, 3868.
- (44) Hiller, D. A.; Singh, V.; Zhong, M.; Strobel, S. A. *Nature* **2011**, *476*, 236.
- (45) Kuhlenkoetter, S.; Wintermeyer, W.; Rodnina, M. V. *Nature* **2011**, *476*, 351.
- (46) Sievers, A.; Beringer, M.; Rodnina, M. V.; Wolfenden, R. *Proc. Natl. Acad. Sci. U.S.A.* **2004**, *101*, 7897.
- (47) Beringer, M.; Bruell, C.; Xiong, L.; Pfister, P.; Bieling, P.; Katunin, V. I.; Mankin, A. S.; Böttger, E. C.; Rodnina, M. V. *J. Biol. Chem.* **2005**, *280*, 36065.
- (48) Rodnina, M. V.; Beringer, M.; Wintermeyer, W. *Trends Biochem. Sci.* **2006**, *32*, 20.
- (49) Beringer, M.; Rodnina, M. V. *Biol. Chem.* **2007**, *388*, 687.
- (50) Schroeder, G. K.; Wolfenden, R. *Biochemistry* **2007**, *46*, 4037.
- (51) Johansson, M.; Bouakaz, E.; Lovmar, M.; Ehrenberg, M. *Mol. Cell* **2008**, *30*, 589.
- (52) Schmeing, T. M.; Huang, K. S.; Strobel, S. A.; Steitz, T. A. *Nature* **2005**, *438*, 520.
- (53) Simonovic, M.; Steitz, T. A. *Biochim. Biophys. Acta* **2009**, *1789*, 612.
- (54) Page, M. I.; Jencks, W. P. *Proc. Natl. Acad. Sci. U.S.A.* **1971**, *68*, 1678.
- (55) Sharma, P. K.; Xiang, Y.; Kato, M.; Warshel, A. *Biochemistry* **2005**, *44*, 11307.
- (56) Trobro, S.; Aqvist, J. *Proc. Natl. Acad. Sci. U.S.A.* **2005**, *102*, 12395.
- (57) Trobro, S.; Aqvist, J. *Biochemistry* **2006**, *45*, 7049.
- (58) Trobro, S.; Aqvist, J. *Biochemistry* **2008**, *47*, 4898.
- (59) Warshel, A. *Computer Modeling of Chemical Reactions in Enzymes and Solutions*; John Wiley & Sons: New York, 1991.
- (60) Das, G. K.; Bhattacharyya, D.; Burma, D. P. *J. Theor. Biol.* **1999**, *200*, 193.
- (61) Suárez, D.; Merz, K. M. *J. Am. Chem. Soc.* **2001**, *123*, 7687.
- (62) Gindulyte, A.; Bashan, A.; Agmon, I.; Massa, L.; Yonath, A.; Karle, J. *Proc. Natl. Acad. Sci. U.S.A.* **2006**, *103*, 13327.
- (63) Massa, L.; Matta, C. F.; Yonath, A.; Karle, J. In *Quantum Biochemistry*; Matta, C. F., Ed.; Wiley-VCH Verlag: Weinheim, 2010; p 501.
- (64) Thirumoorthy, K.; Nandi, N. *J. Phys. Chem. B* **2008**, *112*, 9187.
- (65) Wallin, G.; Aqvist, J. *Proc. Natl. Acad. Sci. U.S.A.* **2010**, *107*, 1888.
- (66) Wang, Q.; Gao, J.; Liu, Y.; Liu, C. *Chem. Phys. Lett.* **2010**, *501*, 113.
- (67) Rangelov, M. A.; Vayssilov, G. N.; Yomtova, V. M.; Petkov, D. D. *J. Am. Chem. Soc.* **2006**, *128*, 4964.
- (68) Tantillo, D. J.; Chen, J.; Houk, K. N. *Curr. Opin. Chem. Biol.* **1998**, *2*, 743.
- (69) Hratchian, H. P.; Schlegel, H. B. *J. Chem. Phys.* **2004**, *120*, 9918.
- (70) Becke, A. D. *J. Chem. Phys.* **1993**, *98*, 5648.
- (71) Zhao, Y.; Truhlar, D. G. *Theor. Chem. Acc.* **2008**, *120*, 215.
- (72) Zhao, Y.; Truhlar, D. G. *Acc. Chem. Res.* **2008**, *41*, 157.
- (73) Gu, J.; Wang, J.; Leszczynski, J.; Xie, Y.; Schaefer, H. F. III *Chem. Phys. Lett.* **2008**, *459*, 164.
- (74) Korth, M.; Grimme, S. *J. Chem. Theory Comput.* **2009**, *5*, 993.
- (75) Sherrill, C. D.; Takatani, T.; Hohenstein, E. G. *J. Phys. Chem. A* **2009**, *113*, 10146.
- (76) Riley, K. E.; Pitonák, M.; Cerny, J.; Hobza, P. *J. Chem. Theory Comput.* **2010**, *6*, 66.
- (77) Riley, K. E.; Pitonák, M.; Jurecka, P.; Hobza, P. *Chem. Rev.* **2010**, *110*, 5023.
- (78) Zhao, Y.; Truhlar, D. G. *J. Chem. Theory Comput.* **2011**, *7*, 669.
- (79) Zhao, Y.; Truhlar, D. G. *Chem. Phys. Lett.* **2011**, *502*, 1.
- (80) Schneebeli, S. T.; Bochevarov, A. D.; Friesner, R. A. *J. Chem. Theory Comput.* **2011**, *7*, 658.
- (81) Thanthiruwatte, K. S.; Hohenstein, E. G.; Burns, L. A.; Sherrill, C. D. *J. Chem. Theory Comput.* **2011**, *7*, 88.
- (82) Papajak, E.; Leverentz, H. R.; Zheng, J.; Truhlar, D. G. *J. Chem. Theory Comput.* **2009**, *5*, 1197.
- (83) Papajak, E.; Truhlar, D. G. *J. Chem. Theory Comput.* **2010**, *6*, 597.
- (84) Papajak, E.; Truhlar, D. G. *J. Chem. Theory Comput.* **2011**, *7*, 10.
- (85) Marenich, A. V.; Cramer, C. J.; Truhlar, D. G. *J. Phys. Chem. B* **2009**, *113*, 6378.
- (86) Marenich, A. V.; Olson, R. M.; Kelly, C. P.; Cramer, C. J.; Truhlar, D. G. *J. Chem. Theory Comput.* **2007**, *3*, 2011.
- (87) Mc Quarrie, D. A. *Statistical Mechanics*; Harper & Row: New York, 1986.
- (88) Frisch, M. J.; et al. *Gaussian 09*, Revision B.01; Gaussian, Inc.: Wallingford, CT, 2009.
- (89) Reed, A. E.; Curtiss, L. A.; Weinhold, F. *Chem. Rev.* **1988**, *88*, 899.
- (90) Altona, C.; Sundaralingam, M. *J. Am. Chem. Soc.* **1972**, *94*, 8205.
- (91) Wiberg, K. A. *Tetrahedron* **1968**, *24*, 1083.
- (92) Kim, Y.; Mohrig, J. R.; Truhlar, D. G. *J. Am. Chem. Soc.* **2010**, *132*, 11071.
- (93) Chalmet, S.; Harb, W.; Ruiz-López, M. F. *J. Phys. Chem. A* **2001**, *105*, 11574.
- (94) Sung, D. D.; Koo, I. S.; Yang, K.; Lee, I. *Chem. Phys. Lett.* **2006**, *426*, 280.
- (95) Ball, P. *Chem. Rev.* **2008**, *108*, 74.
- (96) Kamerlin, S. C. L.; Haranczyk, M.; Warshel, A. *J. Phys. Chem. B* **2009**, *113*, 1253.
- (97) Wilcox, J. L.; Ahluwalia, A. K.; Bevilacqua, P. C. *Acc. Chem. Res.* **2011**, *44*, 1270.
- (98) Cliff, M. J.; Bowler, M. W.; Varga, A.; Marston, J. P.; Szabó, J.; Hounslow, A. M.; Baxter, N. J.; Blackburn, G. M.; Vas, M.; Waltho, J. P. *J. Am. Chem. Soc.* **2010**, *132*, 6507.
- (99) Ditzler, M. A.; Otyepka, M.; Sponer, J.; Walter, N. G. *Acc. Chem. Res.* **2010**, *43*, 40.
- (100) Sponer, J.; Sponer, J. E.; Petrov, A. I.; Leontis, N. B. *J. Phys. Chem. B* **2010**, *114*, 15723.
- (101) Yildirim, I.; Stern, H. A.; Tubbs, J. D.; Kennedy, S. D.; Turner, D. H. *J. Phys. Chem. B* **2011**, *115*, 9261.